scientific reports

Check for updates

OPEN

Peculiar proteome of dark-cultivated *Euglena gracilis*

Adriana Paprčková[1,4], Katarína Klubicová[2,4], Eva Ürgeová[1], Maksym Danchenko[2], Peter Baráth[3], Olha Lakhneko[2], Juraj Krajčovič[1] & Ľubica Uváčková[1]✉

Euglena gracilis **is a flagellate photosynthetic microalga that, thanks to its metabolic adaptability, can grow under both autotrophic and heterotrophic conditions. This adaptability makes euglena an interesting species for applied biotechnology. We focused on the proteome of *E. gracilis* cultivated in Cramer-Myers medium (supplemented with ethanol) in dark and light conditions. Cultures grown in the light showed a characteristic green coloration, while cultures incubated in the dark were bright yellow. When cultured in the dark, microalga showed reduced concentration of chlorophylls (*a*, *b*, and total) and carotenoids compared to cells cultured in the light. Conversely, there was an increase in proline content in the dark compared to light cultivation. Using proteomic approach, we revealed 162 differentially accumulated proteins in light- and dark-grown cells classified into 12 functional groups. Notably, alterations in the metabolism of fatty acids and amino acids, secondary metabolism, and accumulation of stress- and detoxification-related proteins in microalgal cells cultivated in darkness with ethanol as a carbon source may help euglena adapt to these conditions. Based on our results and literature, we hypothesize that vitamin B12 potentially plays an important role in light/dark metabolic switch, similarly as in bacteria.**

Keywords Adenosylcobalamin, B-oxidation of fatty acids, Mixotrophy, Photosynthetic pigments, Proline, Stress

The phylum Euglenozoa represents a widely branched group of unicellular eukaryotic protists[1]. The order Euglenida includes a species-rich group of individually living flagellates characterized by diverse and even unique properties. Among the characteristic features of these protists is the presence of a pellicle composed of parallel protein bands and microtubules, which are located under the cytoplasmic membrane. They ensure cellular plasticity during movement. Type species *Euglena gracilis* (thereupon euglena) is one of the most highly studied eukaryotes because of the ease it can be cultured and its high potential for biotechnology[2].

Inside the cytosol, euglena has a photosensitive receptor—stigma (eyespot) containing derivatives of β-carotene and other carotenoid pigments, which filter light and concentrate it on the paraflagellar body while participating in phototaxis. It reacts to the direction and intensity of light using a photoreceptor located inside the dorsal flagellum[3]. The adaptability of the metabolism allows it to grow in different cultivation conditions, such as autotrophy (using sunlight), heterotrophy (using an external carbon source), and mixotrophy (combining both modes)[4]. Euglena is metabolically versatile thanks to its genome, encoding numerous enzymes and enabling it to utilize various organic compounds as a source of carbon and energy. Most of metabolically active enzymes are regulated post-transcriptionally, allowing cells to adapt quickly to environmental changes[2,5].

Euglena cells change their shape in response to different nutrition and growth conditions. In light-adapted cells, mitochondria are more randomly distributed in the cytosol, with a tendency to localize near the plastids, which may be related to local oxygen production in the plastids[6]. Chloroplasts are easily lost and become permanently bleached under various cultivation conditions. In dark-adapted euglena, the network of mitochondria is located near the surface of the cell and is adjacent to other organelles[6]. These cells contain also undeveloped proplastids, and, after 3 days of exposure to light, they again become developed green chloroplasts[7].

In different cultivation conditions, euglena shows various levels of light harvesting and photosynthesis, which is related to its metabolic pathway. Euglena grown in the light shows an elevated level of pyruvate and a low level of UDP-glucose, glycerate 1-3-bisphosphate, 2-phosphoglycerate, and ATP compared to microalga cultivated in the dark. Euglena grows much faster in the light (mixotrophy) than in the dark (heterotrophy)[4,8] and even faster than under autotrophic conditions due to the limited amount of CO_2[9].

[1]Department of Biology, Institute of Biology and Biotechnology, Faculty of Natural Sciences, University of Ss. Cyril and Methodius in Trnava, Nám. J. Herdu 2, Trnava SK-917 01, Slovakia. [2]Institute of Plant Genetics and Biotechnology, Plant Science and Biodiversity Centre, Slovak Academy of Sciences, Akademická 2, Nitra SK-950 07, Slovakia. [3]Institute of Chemistry, Slovak Academy of Sciences, Dúbravská cesta 9, Bratislava SK-845 38, Slovakia. [4]Adriana Paprčková and Katarína Klubicová contributed equally. ✉email: lubica.uvackova@ucm.sk

Furthermore, microalgae show strong adaptability to various abiotic stresses, constantly fine-tuning their cellular mechanisms to cope with adverse conditions and achieve homeostasis. They accumulate stress metabolites that are closely related to the changes in their metabolic pathways[10]. Light is the most critical environmental factor for the growth of microalgae. High light intensity can significantly increase lipid accumulation in microalgae[11]. One of the first metabolic responses to abiotic stress is inhibition of growth and protein synthesis. As stress becomes more severe, energy metabolism (sugars, lipids, photosynthesis) is affected. Thus, in response to stress, gradual complex changes occur in the metabolism[12].

Polar lipids play an essential role in the structure and fluidity of membranes and are modified by changes in their environment. If the environmental stress acting on the microalgae is mild, only the length of the fatty acid chains and the degree of their deposition will change. On the other hand, if microalgae are exposed to many stresses, the ratio of various polar lipids is modified with higher energy requirements[13].

Chlorophyll *a* is the most widespread pigment in photosynthetic organisms. Chlorophyll *b* is the second most abundant pigment in eukaryotic microalgae and plants. In addition to Chl *a* and Chl *b*, other types of Chls are also known in microalgae *c*, *d*, and *f*. An enhanced Chl *a*/Chl *b* ratio is associated with higher photosynthetic activity and faster cell growth. In unfavorable conditions, the Chl content decreases[14]. Both low light intensity and too high light intensity can have a limiting effect on the growth of microalgae[15]. Light intensity directly affects the rate of photosynthesis. With excessive illumination, microalgae can experience photooxidative damage to the photosynthetic apparatus and photoinhibition—a reduction in the efficiency and speed of photosynthesis[16]. During photoinhibition, increased production of reactive oxygen species (ROS) can occur in cells. In tiny amounts, they fulfill a signaling function and trigger various anti-stress mechanisms, but their high concentrations lead to damage to cellular structures and the transformation of physiological and biochemical processes. As a result of the stress response, there are changes in the composition and ratio of Chls, carotenoids, lipids, and fatty acids[17]. Erickson et al.[16]. reported that high cell density prevents light penetration, which, in turn, reduces the intensity of photosynthesis. In photosynthetic organisms, carotenoids participate in light harvesting and prevent photooxidative damage[18]. Carotenoids are divided into carotenes, oxygen-free pigments, and xanthophylls, oxygen-containing pigments[19]. The most common carotenoids in microalgae are β-carotene and xanthophylls—lutein, violaxanthin, and zeaxanthin[17].

Proline is a multifunctional amino acid and an effective osmoprotectant, which can have a significant role not only in plant development but also in responses to biotic and abiotic stress[20]. The amount of proline reflects a certain physiological state through which we can assess the resilience of plants to stress. It helps microalgae to cope with stress conditions by adjusting the cellular osmotic pressure. Proline contributes to ROS detoxification, membrane integrity, and protein stabilization[21]. Free proline, as well as its end groups in polypeptides, can directly react with hydrogen peroxide and singlet oxygen, neutralizing them. The antioxidant effect of proline is also related to its ability to protect protein-lipid complexes of membranes and indirectly reduce the intensity of lipid peroxidation by inactivating hydroxyl radicals and other ROS. During stress, proline begins to accumulate, its biosynthesis increases, and degradation decreases[22].

The transcriptome datasets, coupled with a draft proteome of *E. gracilis* grown in light and dark conditions, have been generated recently at the descriptive level[23]. The main goal of our work was to monitor the effect of light and dark cultivation of euglena with ethanol as a carbon source on the proteome. This approach can provide a global perspective on the comparison of mixotrophic versus heterotrophic culturing modes. We complemented proteomic data by determining the photosynthetic pigments and proline concentration (stress marker in plants).

Materials and methods

Experimental material and cultivation conditions

Euglena gracilis strain *Z* (Pringsheim strain *Z*, SAG 1224-5/25 Collection of Algae, Göttingen, Germany) was used in this study. Approximately 2×10^6 cells were diluted in Erlenmeyer flasks containing 50 mL of liquid Cramer and Myers (CM) medium[24] supplemented with ethanol (final concentration 0.8%[25]), and pH adjusted to 4.9. The cultures were statically cultivated for 7 days in a cultivation chamber at 23 °C under constant light at an illumination intensity of 30 µmol photons·m^{-2}·s^{-1} and the second part of the cultures was grown under the same conditions in the dark. After 7 days of cultivation, the cells were pelleted by centrifugation at 3350 × *g*, 10 min at 24 °C, and stored at −80 °C until analysis.

Light microscopy

All culture samples were observed under a binocular biological microscope CX23 (Olympus, Hamburg, Germany) at 400-fold magnification. We used 100 µL of formaldehyde to immobilize the cells. Likewise, to observe and compare changes in cellular motility, we observed cells without the addition of formaldehyde in both types of cultures.

Protein extraction and digestion

Proteins were extracted in five independent experiments from both samples (dark and light), according to[26]. Briefly, frozen cells were ground in liquid nitrogen with mortar and pestle. Then 5 mL of extraction buffer (0.1 M Tris–HCl pH 8.8; 10 mM EDTA; 0.9 M sucrose), 20 µL of 2-mercaptoethanol, and 5 mL of basic phenol, pH 8.8 were added. The mixture was placed on a swinging shaker, stirred for 30 min at 4 °C, and then centrifuged at 6000 × *g* at 4 °C for 15 min. Proteins from the phenol phase were precipitated using five volumes of ice-cold 0.1 M ammonium acetate in 100% methanol and incubated overnight at – 20 °C. The precipitate was collected by centrifugation for 20 min, 4000 × *g* at 4 °C. Finally, the pellet was washed 2 times with 0.1 M ammonium acetate in methanol, 2 times with ice-cold 80% acetone, and once with 70% ethanol.

Protein digestion with trypsin on beads was performed according to[27]. Protein samples were solubilized in SDT buffer (4% sodium dodecyl sulfate, SDS; 0.1 M dithiothreitol; 0.1 M Tris-HCl, pH 7.6) at 1000 rpm mixing,

room temperature. Protein concentration was measured using Pierce reducing agent-compatible BCA assay (Thermo Scientific, Waltham, MA USA). 60 µg of protein samples were alkylated with 20 mM iodoacetamide in the dark for 30 min at 24 °C and 600 rpm on thermoshaker TS-100 C (Biosan, Riga, Latvia) and quenched with 5 mM dithiothreitol. Next, the mixture (1:1) of beads was prepared: Sera-Mag Carboxylate-Modified Beads (Cytiva, Marlborough, MA, USA), hydrophilic solids 50 µg/µL, and hydrophobic solids 50 µg/µL. On the magnetic rack MagneSphere (Promega, Madison, WI, USA), the beads were pelleted for 1 min, and the supernatant was removed by pipette. Off the rack, the beads were reconstituted in bidistilled water and pipette mixed. The prepared stock of beads was 20 µg/µL. Following, 30 µL (60 µg) of the bead stock was added to the whole volume of the alkylated/quenched protein sample and pipette-mixed to homogenize the beads and lysate. For binding, 70 µL of 100% ethanol was added to the suspension to achieve 50% final ethanol concentration. The tubes were incubated in the thermoshaker for 10 min at 24 °C and 1000 rpm. On the magnetic rack, the beads were pelleted for 2 min; then, the supernatant was removed and discarded by pipette. Bond proteins were washed 5 times with 140 µL of fresh 80% ethanol.

For digestion, 10 µL of 0.1 µg/µL trypsin (Promega) and 50 µL 50 mM ammonium bicarbonate were added, making the final digestion volume 60 µL. The samples were incubated in the thermoshaker for 18 h at 37 °C and 1000 rpm. On the magnetic rack, the beads were pelleted for 2 min, and the supernatant was recovered into a fresh 2 mL tube, followed by a second elution with 60 µL of 50 mM ammonium bicarbonate. The peptide concentration was measured with a microvolume spectrophotometer DS-11 FX+ (Denovix, Wilmington, DE, USA).

Identification and quantification of proteins by mass spectrometry

Quantitative proteome analysis was done as described earlier[28] 500 ng of purified peptides per sample was loaded onto a trap column (PepMap100 C18, 300 µm × 5 mm, 2-µm particle size, Dionex, Germering, Germany) and separated with an EASY-Spray PepMap RSLC C18 analytical column having integrated nanospray emitter (75 µm × 500 mm, 5-µm particle size) (Thermo Scientific) on Ultimate 3000 RSLCnano system (Dionex) in a 120-min gradient (3–43% of 80% acetonitrile with 0.1% formic acid), and flow rate 250 nL/min. Eluted peptides were sprayed into Orbitrap Elite mass spectrometer (Thermo Scientific), equipped with EASY-Spray ion source, and spectral datasets were collected in the data-dependent mode using Top15 strategy to select precursor ions. Precursors were measured in the mass range 300–1700 m/z with a resolution 120,000, and fragments were obtained by the HCD mechanism with a normalized collision energy 25 and resolution 15,000.

Obtained datasets were processed by MaxQuant v1.6.17.0 with a built-in Andromeda search engine and the following parameters: (i) carbamidomethylation cysteine as permanent and oxidation methionine as variable modifications; (ii) 20 ppm peptide tolerance in the first search, 4.5 ppm in the main search upon recalibration, and 20 ppm fragment tolerance; (iii) 1% peptide and protein false discovery rates based on reverse decoy database search; (iv) match between the runs and label-free quantification (LFQ intensities). The search was performed against euglena translated transcriptome referenced in[23], available in the supporting proteomic dataset at ebi.ac.uk/pride/archive/projects/PXD009998 (36,526 sequences).

The statistical analysis was performed using Perseus v1.6.15.0. Output protein Group table from MaxQuant was filtered for reverse proteins, contaminants, and low-confidence proteins. After the $\log_2$ transformation of the LFQ intensities, only proteins with 4 or more valid values out of 5 biological replicates in any experimental group were retained. Consequently, the missing values were imputed from the normal distribution. Principal component analysis (PCA) was used to evaluate sources of variability among samples and replicates. Next, the Student's test was performed with permutation correction for multiple testing with a q-value threshold at 0.01.

Protein sequences were functionally annotated using BLASTP with an e-value cut-off at 2×10^{-4} querying NCBI non-redundant protein database. Not annotated proteins were additionally searched for predicted protein domains and families using InterPro (ebi.ac.uk/interpro/)[29]. We used eggNOG-mapper for functional enrichment[30] and KEGG-mapper to obtain metabolic pathway map[31].

Determination of the concentration of photosynthetic pigments and proline

The concentration of photosynthetic pigments was determined in 5 independent replicates from each culture (light and dark). From 1 mL of sample, cells were collected by centrifugation at 5800 × g for 5 min and intensively mixed for 2 min in 1mL of 80% (v/v) acetone. After centrifugation at 10,000 × g for 5 min, the concentration of photosynthetic pigments, chlorophylls and carotenoids, was determined spectrophotometrically (Spectroquant UV/VIS Spectrophotometer Pharo 300, Merck, Darmstadt, Germany) at three wavelengths 470 nm, 645 nm, and 662 nm. The concentrations were calculated according to[32].

The proline concentration was determined according to[33] in 3 replicates. We added 1.5 mL of 95% ethanol to each frozen cell sample and thoroughly homogenized with mortar and pestle. After centrifugation for 10 min at 2650 × g room temperature, we added a reaction mixture containing 1% ninhydrin, 20% ethanol, and 60% acetic acid. After intensive mixing for 1 min and incubation at 95 °C for 20 min, we determined the concentration of proline spectrophotometrically based on the calibration curve by measuring the absorbance at 520 nm.

Statistical analysis was done in Excel (Microsoft) using Student's test with a p-value threshold at 0.05.

Results and discussion

Different phenotypes in light versus darkness

As a result of the changed cultivation conditions (light *versus* darkness), we observed the growth of euglena cells in both types of cell cultures but with different coloring. Microalgal cells cultivated in the light showed a typical green coloration, while euglena cells grown in the dark were bright, without the typical green coloration (Fig. 1A-B). Green microalgae absorb light energy through the main photosynthetic pigment chlorophyll *a* (*b*) in the range of 450–475 nm and 630–675 nm[34].

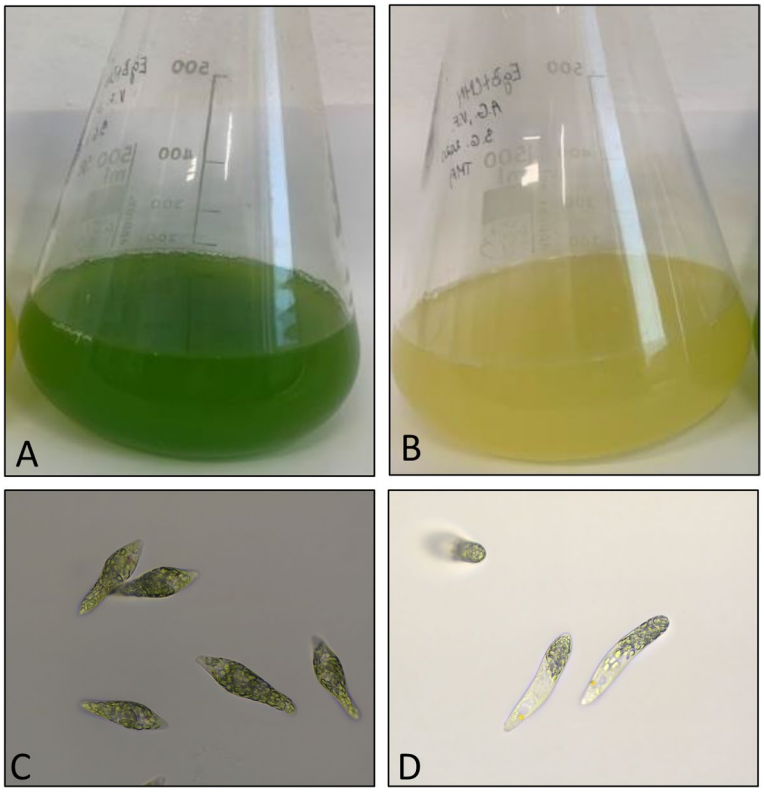

Fig. 1. Phenotype of *Euglena gracilis*. Cultures in light (**A**) and dark (**B**) conditions after 7 days of incubation in Cramer-Meyers medium. Cells cultured in the light showed a characteristic green color, while cells cultured in the dark were yellowish. Microscopy images with 400 × magnification in light (**C**) and dark (**D**) cultivation conditions. Cells cultured in the dark changed shape from oblong to spherical.

Based on microscopic observations, we can conclude, cells cultured in the dark moved significantly slower than those cultured in the light (data not shown). There were visible also significant changes in morphology. Cells cultured in the dark changed shape from oblong to spherical. In the light-grown sample, we noted a higher cellular density (Fig. 1C-D). According to the biological clock, euglena changes its shape twice per day, enacting a circadian rhythm in cell shape. The mean cell length of the population increases to a maximum in the middle of the light period when photosynthetic capacity is highest, and then decreases for the remainder of the 24-hour period. The population becomes spherical by the end of the 24-hour period when the cycle reinitiates[35].

Opposing content of photosynthetic pigments and proline

In cells cultivated in the dark, the concentration of total Chl, Chls *a*/*b*, and carotenoids significantly decreased compared to microalgal cells cultivated in the light. Chlorophyll *a* was reduced at least 40-fold, Chl *b* 3.3-fold, total Chl 24-fold, and carotenoids 3.8-fold in euglena cells cultivated in the dark (Fig. 2A-B). Photosynthetic pigments are essential compounds for energy absorption and conversion in phototrophic organs. An optimal amount of these pigments in the thylakoid membrane is necessary for a balanced energy state and vitality of phototrophs. Cultivation in the dark affected the efficiency of photosynthesis and, thus, cell survival. Azizullah et al.[36]. reported that Chl *b* is more resistant to environmental stresses in euglena than Chl *a* and carotenoids. The ratio Chl *a*/Chl *b* is relatively stable under standard conditions and usually around 3 in the plants[37]. However, when plants are exposed to stress, there can be alterations in this ratio. In our experiments, the ratio Chl *a*/Chl *b* (16.6) was influenced by (light) cultivation conditions.

Middepogu et al.[38] observed a significant decrease in Chl *a*/Chl *b* content in *Chlorella pyrenoidosa* at different concentrations of titanium dioxide nanoparticles. Chlorophyll content decreased with increasing nanoparticle concentration. The shielding effect of nanoparticles can affect photosynthetic productivity due to the reduction of light penetration into algal cells[39]. During cultivation in the dark, there is a significant decrease in the content of Chl in euglena cells. Subsequently, the cells acquire a yellow color, primarily attributed to the presence of carotenoids[40].

We observed an increase in proline content in cultures maintained in the dark compared to cultures grown in the light (Fig. 2C). In the case of cultivation in the light, the proline concentration was 5.6 µg/mL, and in the case of cultivation in the dark, 11.4 µg/mL. As a result of the changed culture conditions, there was a 2-fold increase in proline in cells cultured in the dark compared to the light. Also interesting are the results in *Scenedesmus* sp. exposed to high salt concentration, where a significant increase in proline content was recorded; however, decreased with prolonged exposure to stress, suggesting a possible dynamic regulation of its metabolism[41].

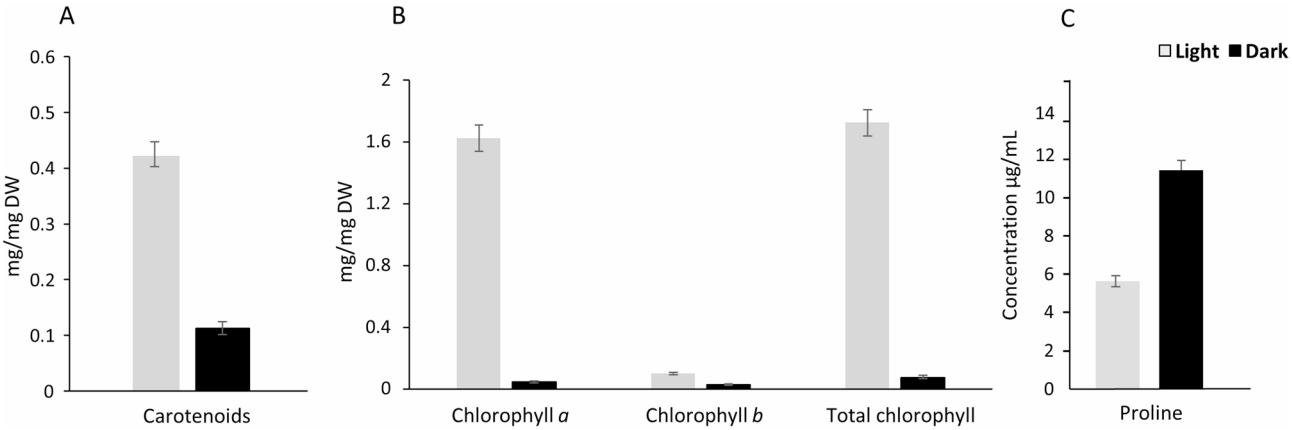

Fig. 2. Concentrations of chlorophylls $n = 7$ (**A**), carotenoids $n = 7$ (**B**), and proline $n = 3$ (**C**) in *Euglena gracilis* cultivated in light (light grey) and dark (black) conditions after 7 days of incubation in Cramer-Meyers medium.

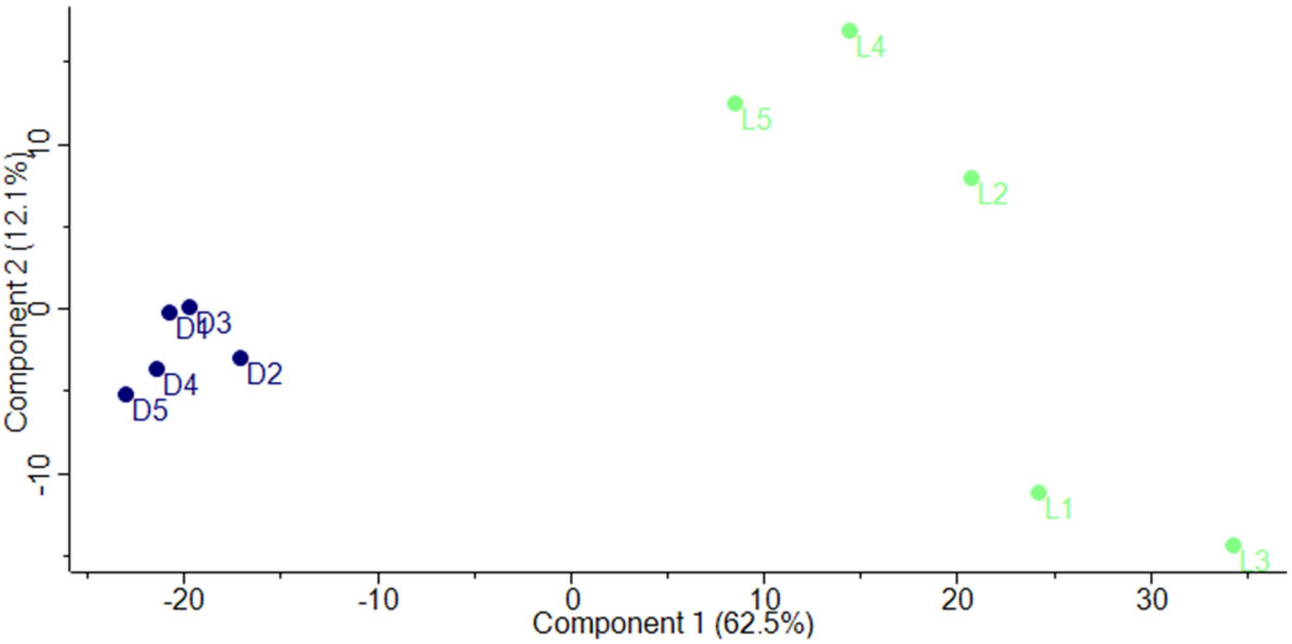

Fig. 3. Principal component analysis of quantified proteins showing separation and distribution of the microalgal samples cultivated in light (green, L1-L5) and dark (blue, D1-D5) conditions. The figure shows 5 independent samples for each variant. The first component, explaining a major share of the total data variance, aligned with different experimental conditions—cultivation in light versus darkness. The second component explained much lower proteome-level variance between biological replicates, particularly in light cultivation.

Mitochondria in euglena are known to contain a higher level of proline[42]. Mitochondrial proline catabolism is linked to oxidative respiration and provides energy for resuming growth after stress[43].

Light-cultivated microalga showed more heterogenic proteome profile

We identified 2449 proteins by mass spectrometry (Table S1). At the 99% confidence level (q-value is 0.01), we revealed 162 differentially abundant proteins (Table S2), classified into 12 functional groups: primary metabolism (23), energy (62), protein destination and storage (13), transcription (3), cell growth and division (4), protein synthesis (11), disease/defence (19), transporters (7), signal transduction (6), secondary metabolism (3), unclear characterization (3). Due to the genetic and metabolic specificity of euglena, some potentially important proteins still remain annotated/uncharacterized (8). Overall, 102 proteins accumulated in the light and 60 in the dark (Table S3). Based on the PCA analysis (Fig. 3), 1st component explained 62% of the total variance in the data, clearly separating experimental groups. Samples cultivated in the dark showed high homogeneity of the

overall protein profile. The group of samples cultivated in the light showed higher heterogeneity aligned with component 2, explaining only 12% of data variance.

Due to the high specificity of euglena genome, we used several tools for the functional annotation of proteins, first we used BLASTP search against the NCBI database (Table S3), InterPro for functional domains, and eggNOG-mapper (Table S4). Finally, we created metabolic maps based on KEGG annotations[30,31] (Fig. 4).

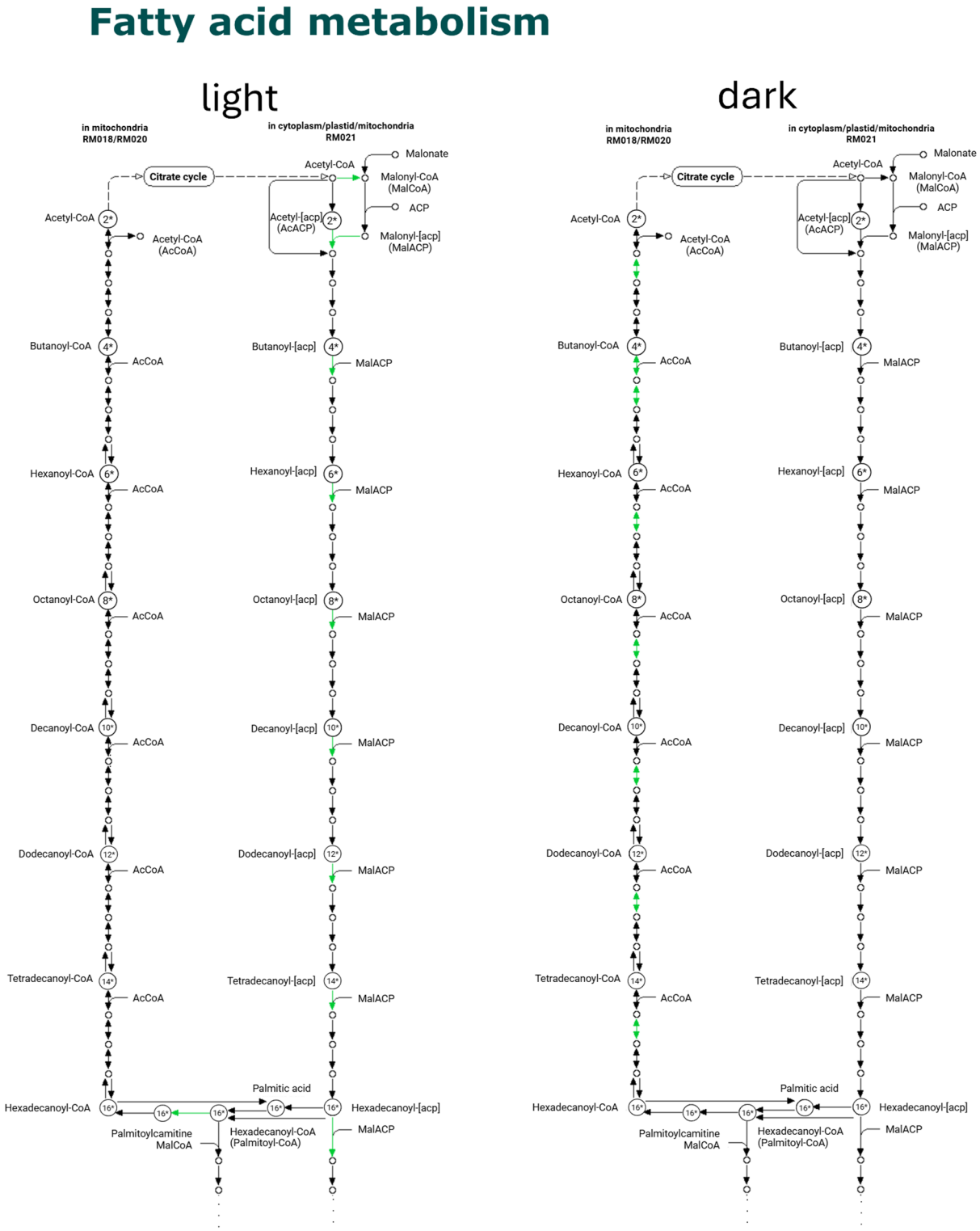

Fig. 4. KEGG-reconstruct assisted visualization of proteomic map of fatty acid metabolism in dark and in light cultivated *Euglena gracilis*. Green arrows represent proteins identified in our study.

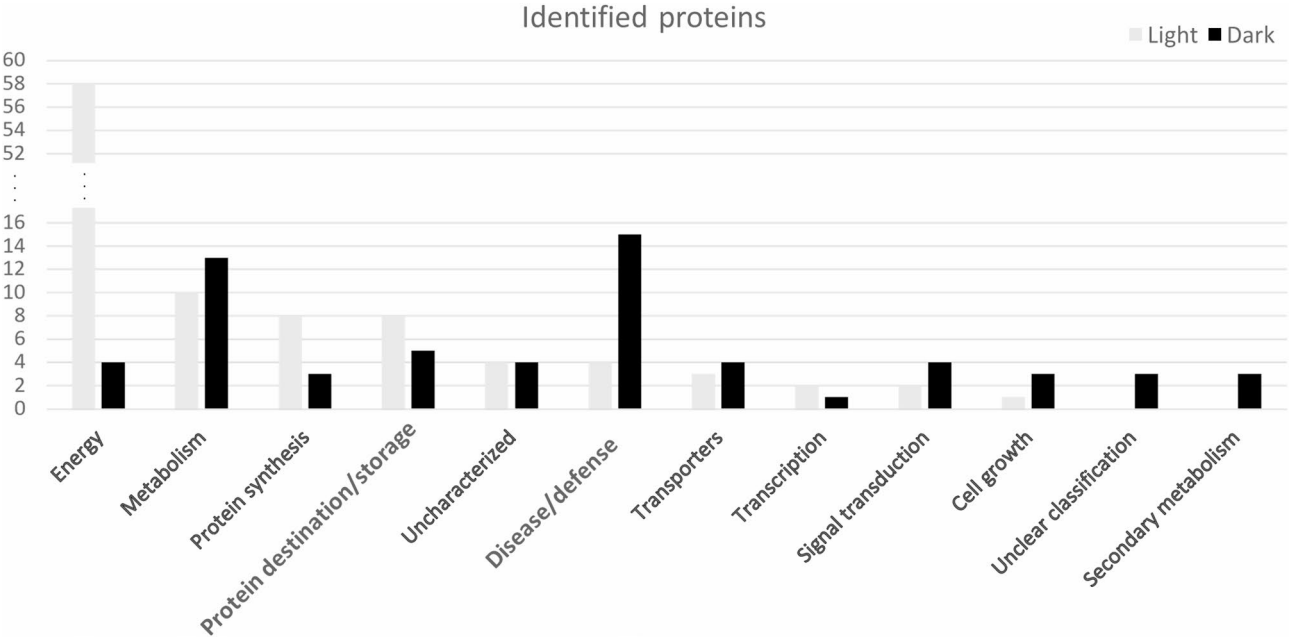

Fig. 5. Functional distribution of differentially abundant proteins accumulated in light (light grey) and dark (black) cultivated *Euglena gracilis*.

The highest difference we observed in the functional groups related to the energy, metabolism of fatty acids and amino acids, defence and antioxidant mechanism (Fig. 5).

When cultivated in the dark with oxygen availability, euglena switches to a heterotrophic way of life, where it relies on various organic substances from the environment as a source of carbon and energy instead of sunlight. In anaerobic or hypoxic conditions, euglena degraded and converted paramylon, the storage polysaccharide, into wax esters, process called wax ester fermentation[44]. High variability was observed even in the level of ability to tolerate hypoxia; some strains can just survive, a few can grow heterotrophically even under anoxia in the dark[45].

Dark cultivation caused the accumulation of numerous defense-related proteins in microalga

We also observed the accumulation of proteins active in stress and detoxification in euglena cultured in the dark. The most represented proteins are 3 entries of glutathione-S-transferases and 2 glutathione transferase (super) family (Table S3), Hsp70 (2 entries more abundant in the dark).

The regulation of ROS is essential for improving plant stress tolerance and is mediated by an antioxidant defense system consisting of several antioxidant enzymes and non-enzymatic antioxidants. Enzymatic antioxidants in microalgae include ascorbate peroxidase (APX), and glutathione-S-transferase. Non-enzymatic antioxidants consist of metabolites such as vitamin C (AsA), glutathione, carotenoids, phenolics, and proline[46]. APX has the ability to synthesize AsA in plants and algae[47]. Water-soluble thiol, glutathione, increases the tolerance of plants to various abiotic stresses, such as cultivation in the dark, and helps keeping ROS under control[48]. Hsp70 (2 entries more abundant in the dark) is a vital chaperone protein involved in protecting cells from stress conditions and helping to maintain protein functions. It binds to damaged and normal proteins and protects them from aggregation and degradation. Hsp70 helps proteins to fold correctly during synthesis or after exposure to stress[49]. In the dark, we identified 7 stress response proteins, while in the light, only 2. Almost the same ratio of identified proteins between dark and light is in the subgroup detoxification, 8:2. Peroxiredoxins (1 accumulated in the dark and 1 in the light) are vital components of the cellular defense against oxidative stress. They catalyze the reduction of peroxides and reduce the level of ROS, thereby protecting and maintaining cellular homeostasis. They may be involved in various cellular processes, including the protection of cell membranes, the regulation of growth, and stress response[50]. Fine details of ROS metabolism still remain unclear in euglena and should be a focus of deep investigation.

Essential changes in amino acid and fatty acid metabolism caused by the absence of light

Among the proteins accumulated in dark-cultured microalga, 8 proteins were involved in the metabolism of amino acids, fatty acids, and sugars (Table S3). We focus on discussing plausible functional implications of the modified amino acids and fatty acids metabolism and secondary metabolism. Amino acid metabolism is crucial for various cellular processes, including DNA and RNA synthesis, energy flows, and signaling pathways. Amino acids can be degraded to tricarboxylic acid cycle intermediates through oxidation. The metabolism of alanine, aspartic acid, and glutamate not only contributes to protein synthesis but also generates intermediates for various metabolic processes. Changes in the metabolism of these amino acids upon exposure to stress can have significant consequences for energy metabolism, redox balance, and production of key metabolites[51].

Aspartate semialdehyde dehydrogenase, accumulated in dark-grown cells, catalyzes the conversion of aspartate semialdehyde to aspartate, a key step in the biosynthesis of the amino acids, lysine, and tyrosine. This enzyme is essential for maintaining the balance of amino acids in euglena cells. Another protein, more abundant in dark conditions, L-aspartate oxidase, catalyzes the conversion of L-aspartate to oxaloacetate in the presence of oxygen, releasing hydrogen[52]. In green algal and plant cells, aromatic amino acids (phenylalanine, tyrosine, and tryptophan) are primarily produced in plastids, but the shikimate pathway functions in both chloroplasts and cytosol. The preferred pathway depends on the conditions of cultivation. The cytosolic pathway dominates when cultured in the dark, and the plastidic pathway is preferential when cultured in the light. Tryptophan is synthesized from chorismate by a series of reactions via anthranilate[9]. In the dark, we revealed the accumulation of anthranilate phosphoribosyltransferase, which catalyzes the second step in tryptophan synthesis. It ensures the transfer of the phosphoribosyl group to anthranilate to form phosphoribosyl anthranilate. Tryptophan synthesis is essential for proper growth and physiological processes[53].

Another essential process affected by dark cultivation is fatty acid metabolism (Fig. 4). In dark cultivated euglena, accumulated proteins active in this process showed chloroplastic localization. In euglena grown in dark accumulated proteins active in fatty acid metabolism localized in mitochondria (L-3-hydroxyacyl-CoA dehydrogenase subunit precursor, acetyl-CoA acetyltransferase (2 entries), known also as thiolases). Mitochondria in euglena are very interesting organelles such as they are facultatively anaerobic and allow to generate ATP both with and without oxygen. One of five systems for fatty acid synthesis occurs in mitochondria – wax ester fermentation[42]. However, the enzymes that accumulated in dark are also active in the β-oxidation of fatty acids in euglena. Together with cytosolic acyl coenzyme A thioester hydrolase isoform X4, which also accumulated in dark, we found 3 of 4 enzymes active in this pathway. Therefore, we interpret that β-oxidation is vital for euglena grown in heterotrophic conditions.

Fatty acid β-oxidation is an important catabolic process providing energy for cells. In the darkness, photosynthesis is not feasible, so cells must rely on alternative energy sources. Activation of acyl-CoA by the enzyme acyl-CoA synthetase initiates β-oxidation in the peroxisomal membrane. The basic reaction of β-oxidation of fatty acids requires a cyclic enzymatic reaction in four steps, namely oxidation, hydration, dehydrogenation, and cleavage of acetyl-CoA. The products of this pathway are acetyl-CoA, NADH, and FAD[6].

Secondary metabolism potentially regulates light/dark metabolic switch

We found enzymes active in secondary metabolism accumulated in euglena grown in the dark. Notably, we found a protein (EG_transcript_16043) that was not functionally annotated in the previous study[23]. However, due to increased data availability, InterPro analysis now showed similarity of this sequence to corrinoid adenosyltransferase PduO-type. This enzyme, accumulated in cells grown in dark, catalyzes the conversion of cobalamin (vitamin B_{12}) into its coenzyme form, adenosylcobalamin ($AdoB_{12}$). This may lead to an increased level of available vitamin B_{12} coenzyme form, which has various regulatory functions in bacteria. As a cofactor, it influences the activity of several enzymes such as isomerases, methyltransferases, and reductases[54]. Adenosylcobalamin, as a part of a specific transcriptional repressor, is involved in down-regulation of a light-inducible promoter in *Myxococcus xynthus*[55]. Finally, photoreceptors use adenosylcobalamin to sense light and mediate light-dependent gene regulation in *Thermus thermophilus*[56,57]. Therefore, we hypothesize that accumulation of this enzyme in dark-grown cells may represent one of mechanisms involved in light/dark metabolic switch in euglena. However, the exact mechanism should be examined.

Finally, spermidine/spermine synthase, active in polyamine (spermidine and spermine) synthesis, also accumulated in dark-grown cells. Polyamines are crucial for cell survival and function. They play essential roles in various cellular processes such as cell growth, cell division, and adaptation to environmental conditions, especially through the protection of cells from oxidative stress[58,59].

Several energy-related proteins accumulated in dark conditions

During cultivation in the dark, we revealed 4 accumulated proteins that belong to the energy category. The main cellular function of β-phosphoglucomutase, exclusive to bacteria and protists, is to catalyze the conversion of β-D-glucose 1-phosphate to β-D-glucose 6-phosphate, which is a universal source of cellular energy and leads to the generation of ATP and NADPH through glycolysis and the pentose phosphate pathway. It also links glycolysis and gluconeogenesis[60] 2,3-biphosphoglycerate-independent phosphoglycerate mutase (gpmA) catalyzes the reversible conversion of 3-phosphoglycerate to 2-phosphoglycerate in glycolysis[61]. The enzyme glucose-6-phosphate 1-dehydrogenase belongs to the pentose phosphate pathway and catalyzes the dehydrogenation of glucose 6-phosphate, contributing to intracellular redox homeostasis[62]. Aldo-keto reductases comprise a large group of NADPH-dependent enzymes that catalyze redox reactions involved in detoxification, biosynthesis, and intermediate metabolism. Aldo-keto reductases reduce aldehydes, ketones, ketosterols, monosaccharides, and prostaglandins and oxidize trans-dihydrodiols of aromatic hydrocarbons and hydroxysteroids. Plants are associated with the aldo/keto reductase family four, related to the detoxification of aldehydes/ketones and xenobiotics to ascorbic acid biosynthesis[63].

Conclusion

Biochemical parameters and proteome profiles of dark-cultivated cells of *Euglena gracilis* compared with light-grown ones indicated that cultures experienced environmental stress. Notably, enhanced proline content and accumulation of defense-related proteins in dark conditions corroborated such idea. Particularly, we detected glutathione-S-transferases, peroxiredoxins, and heat-shock proteins among defense-related proteins. As a part of amino acid metabolism, we highlighted 4 proteins, more abundant in the dark, involved in the metabolism of aspartic acid, tryptophan, and purines. Amino acid metabolism is involved in energy metabolism in plants and is crucial for various cellular processes, including DNA and RNA synthesis, energy flow, and signaling pathways.

During cultivation in the dark, changes in amino acid metabolism might occur because the lack of light affects energy balance and cellular processes. Particular attention deserves fatty acid metabolism. In the dark, we revealed an accumulation of protein involved in the β-oxidation of fatty acids. Under dark culture conditions, photosynthesis does not occur, requiring cells to rely on alternative energy sources. Euglena can oxidize fatty acids to produce ATP, which is essential for survival. We hypothesize that this process is a vital adaptation to heterotrophic cultivation in the dark. Our proteomic results indicate a putative role of adenosylcobalamin in the regulation of light/dark metabolic switch in euglena, similarly as in bacteria. Direct functional verification of hypothesized scenarios will be the subject of follow-up studies.

Data availability

Data AvailabilityThe mass spectrometry raw data and proteomic processing are available in the ProteomeXchange Consortium via the PRIDE partner repository at https://www.ebi.ac.uk/pride/archive/projects/PXD058143 [64].

Received: 26 February 2025; Accepted: 9 July 2025
Published online: 16 July 2025

References

1. Vesteg, M. et al. Comparative molecular cell biology of phototrophic Euglenids and parasitic trypanosomatids sheds light on the ancestor of euglenozoa. *Biol. Rev.* **94**, 1701. https://doi.org/10.1111/brv.12523 (2019).
2. O'Neill, E. C. et al. Euglena in time: evolution, control of central metabolic processes and multi-domain proteins in carbohydrate and natural product biochemistry. *Perspect. Sci.* **6**, 84. https://doi.org/10.1016/j.pisc.2015.07.002 (2015).
3. Barsanti, L. & Gualtieri, P. *Anatomy of Euglena gracilis*. Handbook of Algal Science, Technology and Medicine, s. 61–70, (2020). https://doi.org/10.1016/B978-0-12-818305-2.00004-8
4. Gu, G. et al. Metabolomics revealed the photosynthetic performance and metabolomic characteristics of *Euglena gracilis* under autotrophic and mixotrophic conditions. *World J. Microbiol. Biotechnol.* **38**, 160. https://doi.org/10.1007/s11274-022-03346-w (2022).
5. Hasan, M. T. et al. Comparative proteomics investigation of central carbon metabolism in *Euglena gracilis* grown under predominantly phototrophic, mixotrophic and heterotrophic cultivations. *Algal Res.* **43**, 101638. https://doi.org/10.1016/j.algal.2019.101638 (2019).
6. Zimorski, V., Rauch, C., van Hellemond, J. J., Tielens, A. G. & Martin, W. F. The mitochondrion of *Euglena gracilis*. In *Euglena: Biochemistry, Cell and Molecular Biology. Advances in Experimental Medicine and Biology* Vol. 979 (eds Schwartzbach, S. & Shigeoka, S.) (Springer, 2017). https://doi.org/10.1007/978-3-319-54910-1_2.
7. Chen, Z. et al. Proteomic responses of dark-adapted *Euglena gracilis* and bleached mutant against light stimuli. *Front. Bioeng. Biotechnol.* **10**, 843414. https://doi.org/10.3389/fbioe.2022.843414 (2022).
8. Zeng, M. et al. Fatty acid and metabolomic profiling approaches differentiate heterotrophic and mixotrophic culture conditions in a microalgal food supplement 'euglena'. *BMC Biotechnol.* **16**, 1–8. https://doi.org/10.1186/s12896-016-0279-4 (2016).
9. Inwongwan, S., Kruger, N. J., Ratcliffe, R. G. & O'Neill, E. C. Euglena central metabolic pathways and their subcellular locations. *Metabolites* **9**, 115. https://doi.org/10.3390/METABO9060115 (2019).
10. Paliwal, C. et al. Abiotic stresses as tools for metabolites in microalgae. *Bioresour Technol.* **244**, 1216–1226. https://doi.org/10.1016/J.BIORTECH.2017.05.058 (2017).
11. Singh, R. P. et al. Advancement of abiotic stresses for microalgal lipid production and its bioprospecting into sustainable biofuels. *Sustainability* **15**, 13678. https://doi.org/10.3390/SU151813678 (2023).
12. Pinheiro, C. & Chaves, M. M. Photosynthesis and drought: can we make metabolic connections from available data? *J. Exp. Bot.* **62**, 869–882. https://doi.org/10.1093/jxb/erq340 (2011).
13. Bonnefond, H., Combe, C., Cadoret, J. P., Sciandra, A. & Bernard, O. Potential of microalgae. In *Green Chemistry and Agro-food Industry: Towards a Sustainable Bioeconomy* (ed. Baumberger, S.) 133–153 (Springer, 2024). https://doi.org/10.1007/978-3-031-54188-9_6.
14. Koh, H. G. et al. Heterologous synthesis of chlorophyll b in *Nannochloropsis salina* enhances growth and lipid production by increasing photosynthetic efficiency. *Biotechnol. Biofuels*. **12**, 1–15. https://doi.org/10.1186/s13068-019-1462-3 (2019).
15. Wong, Y. K. Effects of light intensity. Illumination cycles on microalgae *Haematococcus pluvialis* for production of Astaxanthin. *J. Mar. Biol. Aquacult.* **2**, 1–6. https://doi.org/10.15436/2381-0750.16.1083 (2016).
16. Erickson, E., Wakao, S. & Niyogi, K. K. Light stress and photoprotection in *Chlamydomonas reinhardtii*. *Plant. J.* **82**, 449–465. https://doi.org/10.1111/TPJ.12825 (2015).
17. Maltsev, Y., Maltseva, K., Kulikovskiy, M. & Maltseva, S. Influence of light conditions on microalgae growth and content of lipids, carotenoids, and fatty acid composition. *Biology* **10**, 1060. https://doi.org/10.3390/biology10101060 (2021).
18. Tanno, Y. et al. Light dependent accumulation of β-carotene enhances photo-acclimation of *Euglena gracilis*. *J. Photochem. Photobiol B: Biology*. **209**, 111950. https://doi.org/10.1016/j.jphotobiol.2020.111950 (2020).
19. Wan, X. et al. Reprogramming microorganisms for the biosynthesis of Astaxanthin via metabolic engineering. *Prog Lipid Res.* **81**, 101083. https://doi.org/10.1016/j.plipres.2020.101083 (2021).
20. Nowicka, B. Heavy metal–induced stress in eukaryotic algae—mechanisms of heavy metal toxicity and tolerance with particular emphasis on oxidative stress in exposed cells and the role of antioxidant response. *Environ. Sci. Pollut Res.* **29**, 16860–16911. https://doi.org/10.1007/s11356-021-18419-w (2022).
21. Hayat, S. et al. Role of proline under changing environments: a review. *Plant Signal. Behav.* **7**, 1456–1466. https://doi.org/10.4161/psb.21949 (2012).
22. Dubrovna, O. V., Mykhalska, S. I. & Komisarenko, A. G. Using proline metabolism genes in plant genetic engineering. *Cytol. Genet.* **56**, 361–378. https://doi.org/10.3103/S009545272204003X (2022).
23. Ebenezer, T. E. et al. Transcriptome, proteome and draft genome of Euglena gracilis. *BMC Biol.* **17**, 11. https://doi.org/10.1186/s12915-019-0626-8 (2019).
24. Cramer, M. & Myers, J. Growth and photosynthetic characteristics of *Euglena gracilis*. *Archiv Für Mikrobiologie*. **17**, 384–402. https://doi.org/10.1007/BF00410835 (1952).
25. Buetow, D. E. & Padilla, G. M. Growth of *Astasia longa* on ethanol. I. Effects of ethanol on generation time, population density and biochemical profile. *J. Protozool.* **10**, 121–123. https://doi.org/10.1111/j.1550-7408.1963.tb01646.x (1963).
26. Fekecsova, S., Danchenko, M., Uvackova, L., Skultety, L. & Hajduch, M. Using 7 cm immobilized pH gradient strips to determine levels of clinically relevant proteins in wheat grain extracts. *Front. Plant. Sci.* **6**, 433. https://doi.org/10.3389/fpls.2015.00433 (2015).
27. Hughes, C. S. et al. Single-pot, solid-phase-enhanced sample Preparation for proteomics experiments. *Nat. Protoc.* **14**, 68–85. https://doi.org/10.1038/s41596-018-0082-x (2019).

28. Fallah, S. F. et al. Failure in lipid gluconeogenesis, perturbed amino acid metabolism and chaperon activation characterize declined germination potential of aging walnut kernels. *Sci. Hortic.* **329**, 113020. https://doi.org/10.1016/j.scienta.2024.113020 (2024).
29. Paysan-Lafosse, T. et al. InterPro in 2022. *Nucleic Acids Res.* **51**, D418. https://doi.org/10.1093/nar/gkac993 (2023).
30. Cantalapiedra, C. P., Hernández-Plaza, A., Letunic, I., Bork, P. & Huerta-Cepas, J. eggNOG-mapper v2: functional annotation, orthology assignments, and domain prediction at the metagenomic scale. *Mol. Biol. Evol.* **38**, 5825–5829. https://doi.org/10.1093/molbev/msab293 (2021).
31. Kanehisa, M., Sato, Y. & Kawashima, M. KEGG mapping tools for Uncovering hidden features in biological data. *Prot. Sci.* **31**, 47–53. https://doi.org/10.1002/pro.4172 (2022).
32. Lichtenthaler, H. K. & Wellburn, A. R. Determinations of total carotenoids and chlorophylls a and b of leaf extracts in different solvents. *Biochem. Soc. Trans.* **11**, 591–592. https://doi.org/10.1042/bst0110591 (1983).
33. Ahmed, H. & Häder, D. P. Rapid ecotoxicological bioassay of nickel and cadmium using motility and photosynthetic parameters of *Euglena gracilis*. *Environ. Exp. Bot.* **69**, 68–75. https://doi.org/10.1016/j.envexpbot.2010.02.009 (2010).
34. Blair, M. F., Kokabian, B. & Gude, V. G. Light and growth medium effect on *Chlorella vulgaris* biomass production. *J. Environ. Chem. Eng.* **2**, 665–674. https://doi.org/10.1016/j.jece.2013.11.005 (2014).
35. Lonergan, T. A. Regulation of cell shape in *Euglena gracilis*: I. Involvement of the biological clock, respiration, photosynthesis, and cytoskeleton. *Plant. Physiol.* **71**, 719–730. https://doi.org/10.1104/pp.71.4.719 (1983).
36. Azizullah, A., Richter, P. & Häder, D. P. Photosynthesis and photosynthetic pigments in the flagellate *Euglena gracilis*–As sensitive endpoints for toxicity evaluation of liquid detergents. *J. Photochem. Photobiol B: Biology*. **133**, 18–26. https://doi.org/10.1016/j.jphotobiol.2014.02.011 (2014).
37. Lichtenthaler, H. K. et al. Photosynthetic activity, Chloroplast ultrastructure, and leaf characteristics of high-light and low-light plants and of sun and shade leaves. *Photosynth Res.* **2**, 115–141. https://doi.org/10.1007/BF00028752 (1981).
38. Middepogu, A., Hou, J., Gao, X. & Lin, D. Effect and mechanism of TiO_2 nanoparticles on the photosynthesis of *Chlorella pyrenoidosa*. *Ecotoxicol. Environ. Saf.* **161**, 497–506. https://doi.org/10.1016/j.ecoenv.2018.06.027 (2018).
39. Bameri, L., Sourinejad, I., Ghasemi, Z. & Fazelian, N. Toxicity of TiO_2 nanoparticles to the marine microalga *Chaetoceros muelleri* lemmermann, 1898 under long-term exposure. *Environ. Sci. Pollut Res. Int.* **29**, 30427–30440. https://doi.org/10.1007/s11356-021-17870-z (2022).
40. Šantek, B., Friehs, K., Lotz, M. & Flaschel, E. Production of paramylon, a β-1, 3-glucan, by heterotrophic growth of *Euglena gracilis* on potato liquor in fed-batch and repeated-batch mode of cultivation. *Eng. Life Sci.* **12**, 89–94. https://doi.org/10.1002/ELSC.201100025 (2012).
41. Pancha, I. et al. Salinity induced oxidative stress enhanced biofuel production potential of microalgae Scenedesmus sp. CCNM 1077. *Bioresour Technol.* **189**, 341. https://doi.org/10.1016/j.biortech.2015.04.017 (2015).
42. Buetow, D. E. The mitochondrion. In *The Biology of Euglena* Vol. 4 (ed. Buetow, D. E.) 247–314 (Academic, 1989).
43. Viehweger, K. How plants Cope with heavy metals. *Bot. Stud.* **55**, 1–12. https://doi.org/10.1186/1999-3110-55-35 (2014).
44. Inui, H., Ishikawa, T. & Tamoi, M. Wax Ester Fermentation and Its Application for Biofuel Production. *Adv Exp Med Biol* 979, 269–283. (2017). https://doi.org/10.1007/978-3-319-54910-1_13. PMID: 28429326.
45. Tucci, S., Vacula, R., Krajcovic, J., Proksch, P. & Martin, W. Variability of wax ester fermentation in natural and bleached *Euglena gracilis* strains in response to oxygen and the elongase inhibitor Flufenacet. *J. Eukaryot. Microbiol.* **57**, 63–69. https://doi.org/10.1111/j.1550-7408.2009.00452.x (2010).
46. Roy, U. K., Nielsen, B. V. & Milledge, J. J. Antioxidant production in *Dunaliella*. *Appl. Sci.* **11**, 3959. https://doi.org/10.3390/APP11093959 (2021).
47. Wheeler, G., Ishikawa, T., Pornsaksit, V. & Smirnoff, N. Evolution of alternative biosynthetic pathways for vitamin C following plastid acquisition in photosynthetic eukaryotes. *eLife* **4**, e06369. https://doi.org/10.7554/eLife.06369 (2015).
48. Hasanuzzaman, M., Nahar, K., Anee, T. I. & Fujita, M. Glutathione in plants: biosynthesis and physiological role in environmental stress tolerance. *Physiol. Mol. Biol. Plants*. **23**, 249–268. https://doi.org/10.1007/S12298-017-0422-2 (2017).
49. Davoudi, M., Chen, J. & Lou, Q. Genome-wide identification and expression analysis of heat shock protein 70 (HSP70) gene family in pumpkin (Cucurbita moschata) rootstock under drought stress suggested the potential role of these chaperones in stress tolerance. *Int. J. Mol. Sci.* **23**, 1918. https://doi.org/10.3390/IJMS23031918/S1 (2022).
50. Dreyer, A. et al. Function and regulation of Chloroplast Peroxiredoxin IIE. *Antioxidants* **10**, 152. https://doi.org/10.3390/antiox10020152 (2021).
51. Farjallah, A., Roy, A. & Guéguen, C. NMR-and HRMS-based untargeted metabolomic study of metal-stressed *Euglena gracilis* cells. *Algal Res.* **78**, 103383. https://doi.org/10.1016/j.algal.2023.103383 (2024).
52. Kumar, R. et al. Structural–functional analysis of drug target aspartate semialdehyde dehydrogenase. *Drug Discovery Today*. **29**, 103908. https://doi.org/10.1016/j.drudis.2024.103908 (2024).
53. Perveen, S., Rashid, N., Tang, X. F., Imanaka, T. & Papageorgiou, A. C. Anthranilate phosphoribosyltransferase from the hyperthermophilic archaeon *Thermococcus kodakarensis* shows maximum activity with zinc and forms a unique dimeric structure. *FEBS Open. Bio.* **7**, 1217–1230. https://doi.org/10.1002/2211-5463.12264 (2017).
54. Banerjee, R. & Ragsdale, S. W. The many faces of vitamin B12: catalysis by cobalamin-dependent enzymes. *Annu. Rev. Biochem.* **72**, 209–247. https://doi.org/10.1146/annurev.biochem.72.121801.161828 (2003).
55. Pérez-Marín, M. C., Padmanabhan, S., Polanco, M. C., Murillo, F. J. & Elías-Arnanz, M. Vitamin B12 partners the CarH repressor to downregulate a photoinducible promoter in *Myxococcus xanthus*. *Mol. Microbiol.* **67**, 804–819. https://doi.org/10.1111/j.1365-2958.2007.06086.x (2008).
56. Ortiz-Guerrero, J. M., Polanco, M. C., Murillo, F. J., Padmanabhan, S. & Elías-Arnanz, M. Light-dependent gene regulation by a coenzyme B12-based photoreceptor. *PNAS* **108**, 7565–7570. https://doi.org/10.1073/pnas.1018972108 (2011).
57. Jost, M. et al. Structural basis for gene regulation by a B12-dependent photoreceptor. *Nature* **526**, 536–541. https://doi.org/10.1038/nature14950 (2015).
58. Schuber, F., Aleksijevic, A. & Blée, E. Comparative role of polyamines division and plastid differentiation of *Euglena gracilis*. *Biochim. Biophys. Acta (BBA)-General Subj.* **675**, 178–187. https://doi.org/10.1016/0304-4165(81)90224-5 (1981).
59. Mangal, V., Stenzler, B. R., Poulain, A. J. & Guéguen, C. Aerobic and anaerobic bacterial mercury uptake is driven by algal organic matter composition and molecular weight. *Environ. Sci. Technol.* **53**, 157–165. https://doi.org/10.1021/acs.est.8b04909 (2018).
60. Singh, L., Karthikeyan, S. & Thakur, K. G. Biochemical and structural characterization reveals Rv3400 codes for β-phosphoglucomutase in *Mycobacterium tuberculosis*. *Protein Sci.* **33**, e4943. https://doi.org/10.1002/PRO.4943 (2024).
61. Lin, D. et al. Mutation of the rice TCM 12 gene encoding 2,3-bisphosphoglycerate-independent phosphoglycerate mutase affects chlorophyll synthesis, photosynthesis and Chloroplast development at seedling stage at low temperatures. *Plant. Biol.* **21**, 585–594. https://doi.org/10.1111/plb.12978 (2019).
62. Yang, D., Peng, Q., Cheng, Y. & Xi, D. Glucose-6-phosphate dehydrogenase promotes the infection of *Chilli veinal mottle virus* through affecting ROS signaling in *Nicotiana benthamiana*. *Planta* 256, 96; (2022). https://doi.org/10.1007/s00425-022-04010-1
63. Jangra, A. et al. Identification and functional characterization of a novel aldo–keto reductase from *Aloe vera*. *Planta* **258**, 107. https://doi.org/10.1007/s00425-023-04256-3 (2023).
64. Perez-Riverol, Y. et al. The PRIDE database at 20 years: 2025 update. *Nucleic Acids Res.* **6**, 53. https://doi.org/10.1093/nar/gkae1011 (2025).

Acknowledgements
This research was supported by VEGA 1/0230/24 and KEGA 012UCM-4/2025.

Author contributions
Author ContributionsConceptualization, LU; methodology, LU; validation, LU, AP; formal analysis, LU, AP, EU; investigation AP, LU, OL and MD; resources JK; data curation LU, PB, EU; writing—original draft preparation, AP and LU; writing - review and editing, LU, EU, JK, KK and MD; visualization, AP, LU, and MD; supervision, LU; project administration JK; funding acquisition JK. All authors have read and agreed to the published version of the manuscript.

Declarations

Competing interests
The authors declare no competing interests.

Additional information
Supplementary Information The online version contains supplementary material available at https://doi.org/10.1038/s41598-025-11308-z.

Correspondence and requests for materials should be addressed to Ľ.U.

Reprints and permissions information is available at www.nature.com/reprints.

Publisher's note Springer Nature remains neutral with regard to jurisdictional claims in published maps and institutional affiliations.

Open Access This article is licensed under a Creative Commons Attribution-NonCommercial-NoDerivatives 4.0 International License, which permits any non-commercial use, sharing, distribution and reproduction in any medium or format, as long as you give appropriate credit to the original author(s) and the source, provide a link to the Creative Commons licence, and indicate if you modified the licensed material. You do not have permission under this licence to share adapted material derived from this article or parts of it. The images or other third party material in this article are included in the article's Creative Commons licence, unless indicated otherwise in a credit line to the material. If material is not included in the article's Creative Commons licence and your intended use is not permitted by statutory regulation or exceeds the permitted use, you will need to obtain permission directly from the copyright holder. To view a copy of this licence, visit http://creativecommons.org/licenses/by-nc-nd/4.0/.

© The Author(s) 2025